ELSEVIER SCIENCE B.V. [DTD 4.1.0]
JOURNAL OPTMAT ARTICLE No. 109
PAGES 01-6 DISPATCH 9 March 2001
OPTMAT 109
PROD. TYPE: FROM Disk
A

ELSEVIER

Optical Materials 00 (2001) 000–000

OPTICAL Materials

www.elsevier.nl/locate/optmat

Electroluminescence microscopy and spectroscopy of silicon nanocrystals in thin SiO_2 layers

J. Valenta [a,b], N. Lalic [a], J. Linnros [a,*]

[a] *Department of Electronics, Royal Institute of Technology, Electrum 229, S-164 40 Kista–Stockholm, Sweden*
[b] *Faculty of Mathematics and Physics, Department of Chemical Physics and Optics, Charles University, Ke Karlovu 3, Prague 2, CZ-121 16 Czech Republic*

Received 30 May 2000

Abstract

Stable continuously operable electroluminescent diodes have been fabricated by Si^+-ion implantation and annealing of thin SiO_2 layers on a silicon substrate. The external quantum efficiency of the device is reaching 3×10^{-5} for the best diodes. Electroluminescence (EL) emission band is wide and centered at 800 nm. EL is due to radiative recombination of tunneling carriers in Si-nanocrystals(NC) with small contribution of oxide defects (peak at 650 nm). EL images reveal inhomogeneous emission structures on the micrometer scale. Mainly, a small number of bright spots with diffraction limited size (~600 nm) with a homogeneous background are observed and their EL spectra measured using an imaging spectrometer with a liquid-nitrogen-cooled CCD camera. The bright EL spots originate from the efficiently excited emission of oxide defects and/or emission of a few (possibly single) Si-NC, most likely at places with locally increased current. The low efficiency is probably a consequence of current tunneling through optically inactive nanocrystals or defects in a very thin oxide layer. © 2001 Published by Elsevier Science B.V.

Keywords: Nanocrystals; Electroluminescence; Photoluminescence; Implantation; LED

1. Introduction

Light emission from silicon-based materials has been studied extensively during the last decade [1]. The main driving force for this research is the possible fabrication of Si light-emitting-devices (LED) or displays by methods compatible with the present microelectronic technology. There are several possibilities to fabricate Si-based electroluminescent devices: using quantum confinement effects in Si-nanocrystals (NC) [2] or nanowires, doping of Si with rare-earth atoms (e.g., Er^{3+}) [3] or making multiple quantum wells or supperlattices [4,5]. First efficient LEDs were fabricated from porous silicon. They achieved relatively high external quantum efficiency ($>10^{-3}$) but the fast degradation remained a severe drawback [6]. Another approach is to use stable and well passivated Si-NCs in SiO_2 matrix. These structures are made mainly by annealing of CVD deposited Si-rich SiO_2 or by Si^+-ion implantation of SiO_2, which is a method fully compatible with the VLSI technology. In order to obtain a good injection of carriers through the insulating oxide to the NCs it is necessary either (i) to make very high-concentration of Si-NCs (close to the percolation

* Corresponding author. Tel.: +46-8-752-14-22; fax: +46-8-752-77-82.
E-mail address: jan.linnros@ele.kth.se (J. Linnros).

0925-3467/01/$ - see front matter © 2001 Published by Elsevier Science B.V.
PII: S0925-3467(01)00019-2

threshold) and use high voltages or (ii) to make a very thin layer of SiO_2 containing Si-NCs and use tunneling transport through the oxide at low voltages. We have chosen the latter approach and prepared LEDs based on Si nanocrystals grown (by Si^+-ion implantation and annealing) in a thin SiO_2 layer placed between a p-type Si substrate and an n-type poly-Si layer.

The aim of the present work was to study electroluminescence (EL) spectra from Si-NC LEDs using a very sensitive imaging spectrometer, to measure EL spectra with high spatial resolution (detection of spectra of EL from diffraction limited spots of the sample – i.e., full-width in half-maximum (FWHM) of about 0.6 μm) and find a reason for the relatively low external quantum efficiency (max. 3×10^{-5}) of these devices.

2. Experimental

Samples were prepared by a procedure described in [7]. Thermal oxide layers (thickness of 12, 18, 50 or 100 nm) were grown on p-type (1 0 0) Si wafers (resistivity 20 Ω m) and covered by a 210 nm thick amorphous Si layer. Then a dose of 0.3, 1 or 3×10^{17} cm^{-2} of $^{28}Si^+$-ions was implanted at 150 keV. Si-NCs were formed from excess Si in SiO_2 by annealing samples at 1100°C in N_2 atmosphere for 1 h. In order to improve electron injection into the NC a 160 nm thick poly-Si layer highly doped with phosphorus was deposited on top of samples. The final circular shape of diodes was defined by reactive ion etching.

EL and photoluminescence (PL) images and spectra of our diodes were studied using an imaging spectrometer (Spex Triax 190) connected to an optical microscope. The light from the sample was collected by an objective (highest magnification 100×, NA 0.7), imaged on the entrance slit of the spectrometer and detected by the LN-cooled CCD camera (Hamamatsu C4880) attached to the output of the spectrometer. For each sample, first, the image of EL was obtained using a mirror instead of the grating inside the spectrometer (entrance slit opened to maximum). Then, an area of interest was placed in the center of the image, entrance slit closed to desired width (resolution) and the mirror was switched to a diffraction grating (mirror and two gratings are mounted on a same turret) in order to record a spectrum. The set-up allows us to detect a spectrum from any diffraction limited spot (diameter about 500 nm) of the sample. PL was excited by the frequency-doubled output (532 nm) of a Nd:YAG laser (pulse duration of 3 ns, repetition rate about 40 Hz) sent to the sample through an optical fiber. All spectra were corrected for spectral sensitivity of the detection system.

3. Results and discussion

3.1. Spatially integrated EL and PL spectroscopy

The fabricated structures with oxide thickness of 12 and 18 nm emit light under a continuous forward bias at room temperature. The EL intensity

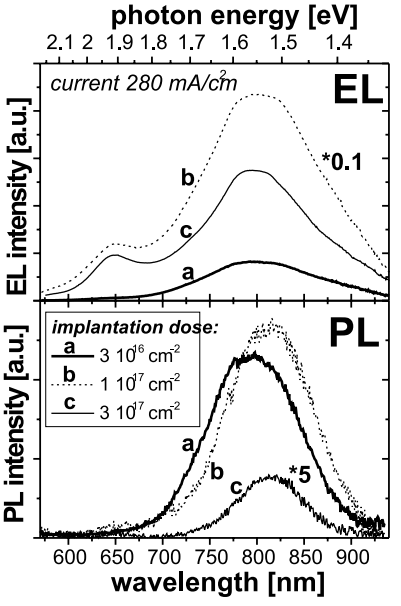

Fig. 1. EL and PL spectra for diodes with 12 nm thick oxide and implantation doses 0.3, 1 and 3×10^{17} cm^{-2} (bold (a), dashed (b) and narrow line (c), respectively). EL spectra are compared for a current density of 280 mA/cm^2. PL was excited with frequency-doubled output of a pulsed Nd:YAG laser (532 nm, 40 Hz, 3 ns, intensity ~1 mJ/cm^2) through the top poly-Si contact.

is very stable and visible by a naked eye for the best diodes.

We will first discuss spatially averaged spectra, collected from a 1 mm^2 area of the diode surface. Fig. 1 (upper panel) compares the EL spectra for samples with 12 nm thick oxide and different implantation doses. Two EL bands are observed peaking around 650 and 800 nm. The relative intensity of the narrower short-wavelength peak is increasing with implantation dose and can be attributed to emission from oxide defects [8]. The main wide EL band around 800 nm is most probably due to emission from Si-NCs. It corresponds well to the PL spectra measured in the same diodes under pulsed excitation through the top poly-Si contact. The 650 nm peak is not observed in the PL probably because it is not efficiently excited by the green light. The PL emission band is somewhat narrower than EL and agrees with the typical PL of similar samples made by Si^+-ion implantation of SiO_2 [9]. The decay of both PL and EL emission is long (10s of μs) and non-exponential (well described by a stretch-exponential curve) [7].

For both EL and PL the highest intensity is emitted from the diode implanted by the dose of 1×10^{17} cm^{-2}. We measured the external quantum efficiency of this diode and found the maximal value of 3×10^{-5}.

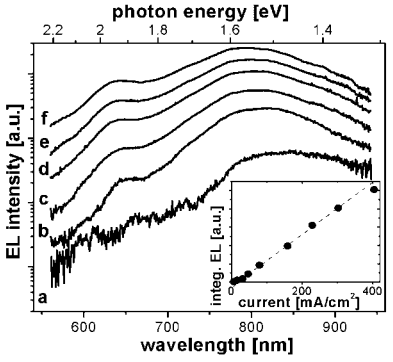

Fig. 2. DC current-dependence of EL spectra of a diode with 18 nm thick oxide, implanted to a dose of 1×10^{17} cm^{-2}. Current densities are 7, 32, 64, 103, 190 and 300 mA/cm^2 for spectra a to f (applied bias was 5–15 V). The inset shows increase of the integrated EL intensity with current.

The current-dependence of the EL spectra and integrated intensity is shown in Fig. 2. The EL intensity increases linearly with current density in the range 30–300 mA/cm^2. It means that the quantum efficiency is constant except for very low-currents (bias up to about 5–6 V) and for very high-currents where saturation regime starts close to the breakdown at high-voltages (around 14 V). The position of the EL peak is slightly shifting towards shorter wavelengths with increasing bias. This is because the injection of carriers into NCs of smaller size (emitting at shorter wavelengths) demands higher bias as the band-gap is increasing with decreasing size of NCs.

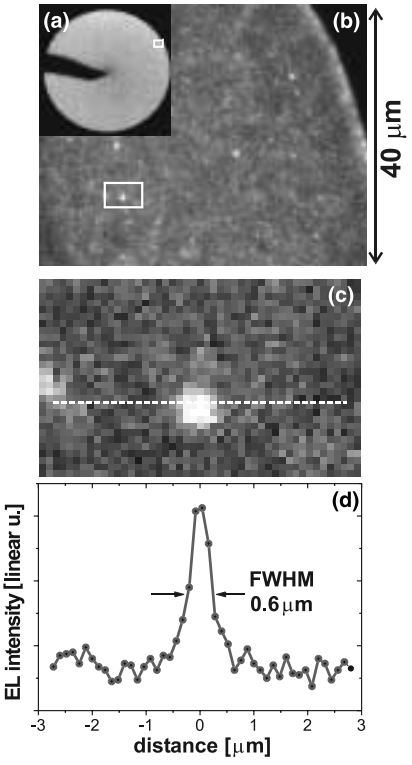

Fig. 3. The EL image of the whole (a) diode (2 mm diameter, oxide thickness 12 nm, dose 1×10^{17} cm^{-2}) with an enlarged detail of 50 × 40 μm area (b). Panel (c) shows the EL image (5.8 × 3.6 μm, one pixel represents an area of 0.12^2 μm) of one bright spot indicated by a white rectangle in (b). The intensity profile of this dot is plotted in the bottom part of the figure.

3.2. EL imaging and highly spatially resolved EL spectroscopy

The EL emission of whole diodes appears homogeneous (Fig. 3(a)), but high-resolution images of EL (Fig. 3) reveals some structures on a micrometer scale. Mainly, a small number of very bright and stable shining spots (Fig. 3(b), (c)) of diffraction limited size ($d = 1.22\lambda/2/\mathrm{NA}$, for wavelength $\lambda = 700$ nm, d is about 600 nm, see Fig. 3(d)) is observed in every diode. Using an imaging spectrometer we were able to detect EL spectra from these single bright spots of the diode. Six different single-spot EL spectra are plotted in Fig. 4. Spectra are often composed of a peak around 640 nm (see Fig. 4, spectrum f, and also b, c, e), and another one peaking between 710–820 nm (i.e., within the main EL band). The spectral features are slightly narrower (FWHM 60–100 nm) than for spatially averaged EL emission bands (FWHM ~150 nm) and their peak positions differ from point-to-point.

We will now concentrate on the discussion of the origin of the bright spot emission. It is evident that for a thin oxide layer (12–18 nm) local fluctuations of layer thickness and of the Si-NC size of the order of few nanometers will create preferential paths for the tunneling current [10]. Thus the current density will be inhomogeneously distributed in the diode and a NC (or defect) located in the high-current path could be efficiently excited. On the other hand, current could pass through defects or optically inactive NCs without contributing to the emission of the diode and thus decreasing the device efficiency.

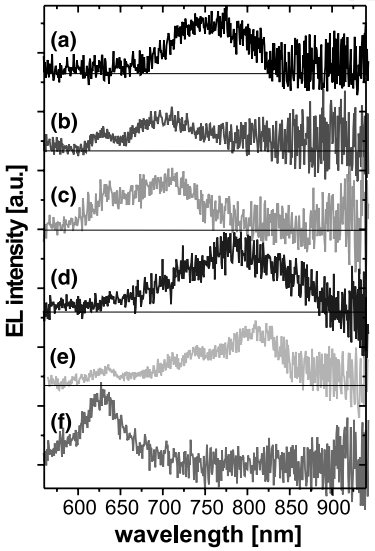

Fig. 4. EL spectra of six different single bright spots of diodes (oxide thickness: (a) 18, (b–f) 12 nm, dose: (a–e) 1×10^{17}, (f) 3×10^{17} cm^{-2}) each accumulated for 30 min (spectral resolution is about 7 nm).

Let us estimate the mean distance of Si-NCs in the oxide layer. According to Monte-Carlo simulations [11], using the TRIM code, an implantation dose of 1×10^{17} cm^{-2} creates a peak excess concentration of Si in SiO_2 of about 10 at.%, i.e., 5×10^{21} cm^{-3}. The TEM observations of similar implanted structures show that the mean diameter of NCs is about 3 nm [12]. This gives us a mean distance between NCs of about 5 nm. But the TEM images revealed also that excess Si atoms precipitate on the Si/SiO_2 interface, which effect will cause significant losses of Si for thin oxide layers (diffusion length of Si for a 1 h annealing at 1100° C is estimated to $L \sim 6.8$ nm). Therefore, the real inter-NC distance is probably significantly longer than 5 nm. Another point is that some Si-NCs are not emitting light due to the presence of non-radiative centers. Starting from Credo's et al. finding that the majority of NCs in a porous-Si sample does not emit light but a few of them (~1%) approach 100% efficiency [13], we can do the following estimation for the concentration of ideally efficient Si-NCs. Let us suppose that our sample contains a single layer of NCs which has either 0 or 100% efficiency of emission and that the emission of photons from one NC takes place with a frequency 10^4 Hz corresponding to a PL lifetime of 100 μs. Then, for a sample with external quantum efficiency of 1×10^{-5} (and estimating that internal efficiency to be 30 times higher), the current of 2 mA/mm^2 creates 3.75×10^{14} photons/s/cm^2, which will correspond to the emission of about 4×10^{10} ideal NCs per cm^2 yielding a mean distance 50 nm between them. This is clearly an upper limit since (a) the injection frequency into a single NC may be lower than 10^4 Hz and (b) the efficiency of each NC could be lower than 100%. In such a case a diffraction

limited spot from the diode always contains at least of the order of ~100 of emitting NCs, which leads to the apparent homogeneity of the EL image. Consequently, EL inhomogeneities should originate from current inhomogeneities, which causes non-uniform excitation rate of NCs.

Concerning the shape of the observed single-spot EL spectra, we have to mention its striking resemblance with PL spectra of single porous-Si grains observed at room temperature by Mason et al. [14]. Also the total number of counts detected in one single-spot EL spectrum roughly corresponds to the signal we expected from ideal single Si-NC taking into account the sensitivity of our detection system. Unfortunately, we cannot provide any direct evidence, that our spectra are the single Si-NC EL spectra. The on–off blinking typical for emission from single NCs [14,15] and molecules cannot be observed in our experiment as the acquisition time for one spectrum is 30 min. Also the proof of single NC origin of emission using the photon-correlation measurement is not possible, as the signal is extremely low. However, the slightly narrower spectra with different peak positions seen in Fig. 4 indicate that we are able to detect spectra from only a few NCs, possibly from single NCs. Indeed, the spectral shape of emission from a single NC could be broad as several luminescence centers could be active [16].

4. Conclusions

EL spectra spatially integrated over 1 mm^2 of diode surface shows a characteristic wide-band emission around 800 nm, which is usually attributed to the radiative recombination in Si-NCs. The peak position shifts slightly to shorter wavelengths with increasing bias. This emission band is observed also in PL spectra. Moreover, weaker emission from oxide defects can be observed in EL spectra around 650 nm.

Magnified EL images reveal small inhomogeneities, mainly a small number of bright spots which have diffraction limited size. The spectra of EL emitted from these spots were successfully detected. Comparing the single-spot EL spectra with the only known PL measurements of single porous-Si grains and estimating the number of Si-NC in these diodes, we can explain bright spots to be due to a locally increased current density which causes a higher rate of emission from oxide defects and/or a few (possibly single NC) Si-NCs laying in the current path. It seems that the number of such current drains is much higher than the number of bright spots, but most of them go through non-radiating (dark) NCs or defects. Such current losses are most likely the reason for the relatively low-external quantum efficiency of our devices ($\leqslant 3 \times 10^{-5}$).

We conclude that the light-emitting-diodes based on very thin SiO_2 layer (<20 nm) containing Si-NCs can operate at low voltages in continuous regime with high stability. The total emission is, however, small due to a small amount of active material and the efficiency is reduced by the non-radiative leakage of current through the oxide.

Acknowledgements

The authors are grateful to T. Pihl for performing the ion implantation. The work was supported by a grant from the faculty of the Royal Institute of Technology. JV acknowledges the support from GACR No. 202/98/0669.

References

[1] D.J. Lockwood (Ed.), Light Emission From Silicon: From Physics to Devices, Academic Press, San Diego, 1998.
[2] J. Linnros, N. Lalic, Appl. Phys. Lett. 66 (1995) 3048.
[3] G. Franzo, S. Coffa, F. Priolo, C. Spinella, J. Appl. Phys. 81 (1997) 2784.
[4] K. Chen, M. Wang, W. Shi, L. Jiang, W. Li, J. Xu, X. Huang, J. Non-Cryst. Solids 198–200 (1996) 833.
[5] S. Chan, P. Fauchet, Appl. Phys. Lett. 75 (1999) 274.
[6] N. Lalic, J. Linnros, J. Appl. Phys. 80 (1996) 5971.
[7] N. Lalic, J. Linnros, J. Lumin. 80 (1999) 263.
[8] J. Yuan, D. Haneman, J. Appl. Phys. 86 (1999) 2358.
[9] J. Linnros, N. Lalic, A. Galeckas, V. Grivickas, J. Appl. Phys. 86 (1999) 6128.
[10] Y. Inoue, A. Tanaka, M. Fuji, S. Hayashi, K. Yamamoto, J. Appl. Phys. 86 (1999) 3199.
[11] N. Lalic, Light Emitting Devices Based on Silicon Nanostructures, Ph.D. thesis, Stockholm, 2000.
[12] J. Linnros, A. Galeckas, A. Pereaud, N. Lalic, V. Grivickas, L. Hultman, Mat. Res. Symp. Proc. 486 (1998) 249.

[13] G.M. Credo, M.D. Mason, S.K. Burrato, Appl. Phys. Lett. 74 (1999) 1978.
[14] M.D. Mason, G.M. Credo, K.D. Weston, S.K. Burrato, Phys. Rev. Lett. 80 (1998) 5405.
[15] N. Banin, M. Bruchez, A.P. Alivisatos, T. Ha, S. Weiss, D.S. Chemla, J. Chem. Phys. 110 (1999) 1195.
[16] M.V. Wolkin, J. Jorne, P.M. Fauchet, G. Allan, C. Delerue, Phys. Rev. Lett. 82 (1999) 197.